

J.P. Davis · H. Choi · J. Pollanen ·
W.P. Halperin

High frequency sound in superfluid $^3\text{He-B}$

Version March 13, 2022

Abstract We present measurements of the absolute phase velocity of transverse and longitudinal sound in superfluid $^3\text{He-B}$ at low temperature, extending from the imaginary squashing mode to near pair-breaking. Changes in the transverse phase velocity near pair-breaking have been explained in terms of an order parameter collective mode that arises from f -wave pairing interactions, the so-called $J = 4^-$ mode. Using these measurements, we establish lower bounds on the energy gap in the B-phase. Measurement of attenuation of longitudinal sound at low temperature and energies far above the pair-breaking threshold, are in agreement with the lower bounds set on pair-breaking. Finally, we discuss our estimations for the strength of the f -wave pairing interactions and the Fermi liquid parameter, F_4^s .

Keywords superfluid · helium · collective mode · pair-breaking · transverse sound · longitudinal sound

PACS 67.30.H- · 74.20.Rp · 74.25.Ld · 43.35.Lq

J.P. Davis
Department of Physics and Astronomy, Northwestern University, Evanston, IL
60208, USA
Tel.: 780-248-1410
E-mail: jdavis@ualberta.ca
Present address: J.P. Davis, Department of Physics, University of Alberta, Edmon-
ton, Alberta T6G 2G7, Canada

W.P. Halperin
Department of Physics and Astronomy, Northwestern University, Evanston, IL
60208, USA
Tel.: 847-491-3686
E-mail: w-halperin@northwestern.edu

1 Introduction

In 1957 Landau [1] predicted the existence of new collective modes of a degenerate Fermi liquid in the high frequency and low temperature limits where local thermal equilibrium cannot be established. One of these so-called zero sound modes, the longitudinal mode, was observed by Abel *et al.* [2] in 1966. The second predicted zero sound mode was transverse sound. It is intriguing that the conditions on shear stiffness that are required for propagation of a transverse wave might be satisfied in a liquid, and in particular in the Fermi liquid ^3He . Nonetheless, the second mode predicted by Landau has never been observed [3]. Moores and Sauls [4] pointed out that transverse sound might propagate at low temperatures in the B-phase of superfluid ^3He as a consequence of its coupling to the imaginary squashing mode (ISQ), a well-established collective mode of the order parameter. They predicted a significant increase in the velocity owing to an off-resonant coupling with the ISQ which would significantly enhance the observability of transverse sound. The phenomenon was observed by Lee *et al.* [5] exploiting an acoustic Faraday effect to unambiguously demonstrate that the propagating mode they discovered had transverse polarization. According to the theory and subsequent experimental work [4,5,6,7,8], we know that this coupled transverse mode propagates only at frequencies between that of the ISQ-mode, shown as the blue curve in Fig. 1, and pair breaking, the black curve. In the present work we investigate the region near the pair breaking threshold in superfluid ^3He exploiting both transverse and longitudinal sound modes using acoustic cavity interference methods.

We recently reported observation of a new collective mode near the pair-breaking energy, 2Δ , based on anomalies in phase velocity, attenuation and acoustic birefringence of transverse sound [8]. The additional measurements we present here are made possible by improvements in acoustic techniques, notably acoustic cavity interferometry and pressure sweeps at low temperature. Our measurements of this mode establish a lower bound for the energy gap, Δ , since the energy, $\hbar\omega$, of the 2Δ -mode is close to, but below, the pair-breaking threshold, 2Δ . Previous reports of the pair-breaking threshold based on longitudinal sound attenuation [9,10] are difficult to reconcile with theory since they give values (at low pressure) less than BCS weak-coupling. In the pressure range from 1 to 20 bar, we find that the gap always lies above weak-coupling values. Additionally, we compare measurements of longitudinal sound with transverse sound. We find that longitudinal sound continues to propagate at energies far above 2Δ , albeit with significantly high attenuation. From longitudinal sound attenuation we extract the threshold energy for pair-breaking at 3.7 bar, consistent with the lower bounds established by the 2Δ -mode.

Selection rules for the coupling between transverse sound and order parameter collective modes provide the basis for our identification of the 2Δ -mode as having total angular momentum $J \geq 4$. A $J = 4$ mode has been predicted to exist if there is an attractive, sub-dominant f -wave pairing interaction [11]. There have been predictions for sub-dominant pairing interactions in high T_c superconductors [12] and in superfluid ^3He [11,13]. Superfluid ^3He

is a spin triplet, p -wave pairing condensate where the possible role of f -wave interactions has been the subject of considerable interest both experimentally and theoretically. Several experiments, including magnetic susceptibility [14, 15] and spectroscopy of the ISQ and real squashing (RSQ) collective modes [3, 6, 7, 16, 17, 18], have been analyzed to try and determine the f -wave pairing interaction, as well as Fermi liquid interactions, in an effort to predict the $J = 4$ mode frequency. However, the results of these different analyses are ambiguous owing to imprecision of the Fermi liquid parameters, $F_2^{a,s}$, as well as non-trivial strong coupling contributions to the ISQ-mode frequencies [7]. The strength of the f -wave pairing interactions can be estimated from the 2Δ -mode energies in terms of the theory [13] if assumptions are made about the high order Fermi liquid parameter, F_4^s . Conversely, we can estimate F_4^s using independent values for the f -wave pairing strength, taken from measurements of another order parameter collective mode, the RSQ. It is traditional to refer to these modes by their total angular momentum, J , and to indicate explicitly their parity under particle-hole conversion. Then the ISQ is called the $J = 2^-$ mode, the RSQ is the $J = 2^+$ mode and the new mode, as predicted, would be $J = 4^-$. Particle-hole symmetry is relevant to the strength of the coupling of order parameter collective modes to sound [3, 19]. For example, for perfect particle-hole symmetry, which is the case of even parity, there can be no coupling to the RSQ-mode.

2 Longitudinal and Transverse Acoustic Response

The experimental arrangement is described in Refs. [7, 8]. We form an acoustic cavity with a spacing of $D = 31.6 \pm 0.1 \mu\text{m}$ between an AC -cut transducer (6 MHz fundamental frequency) and an optically polished quartz reflector. The temperature is held fixed near ≈ 0.5 mK and the pressure is swept while keeping the acoustic frequency, ω , constant. The energy gap, Δ , is dependent on the pressure and therefore a decreasing pressure sweep changes the relative energy of the acoustic waves to the energy gap, as well as to the order parameter collective modes, shown schematically by the red arrow in Fig. 1. Specifically, we use the weak-coupling-plus energy gap of Rainer and Serene [20], referenced to the Greywall temperature scale [21]. The low temperature pressure sweep method results in crossing the 2Δ -mode at $T/T_c = 0.29$ at a pressure of 19.4 bar (170 MHz), up to $T/T_c = 0.53$ for 1.2 bar (76 MHz).

The acoustic response, V_Z , was detected using a cw-impedance bridge [22], which is sensitive to changes in the standing wave condition of the sound wave in the cavity through changes in the electrical impedance of the transducer. The transverse acoustic response is given by

$$V_Z = a + b \cos \theta \sin \left(\frac{2D\omega}{c} + \phi \right). \quad (1)$$

The angle θ is the direction of polarization of the sound wave at the surface of the transducer relative to the polarization of the shear transducer; c is the sound velocity and ϕ is a fixed phase that depends on experimental conditions. This is superposed on a slowly varying background, a , not shown in

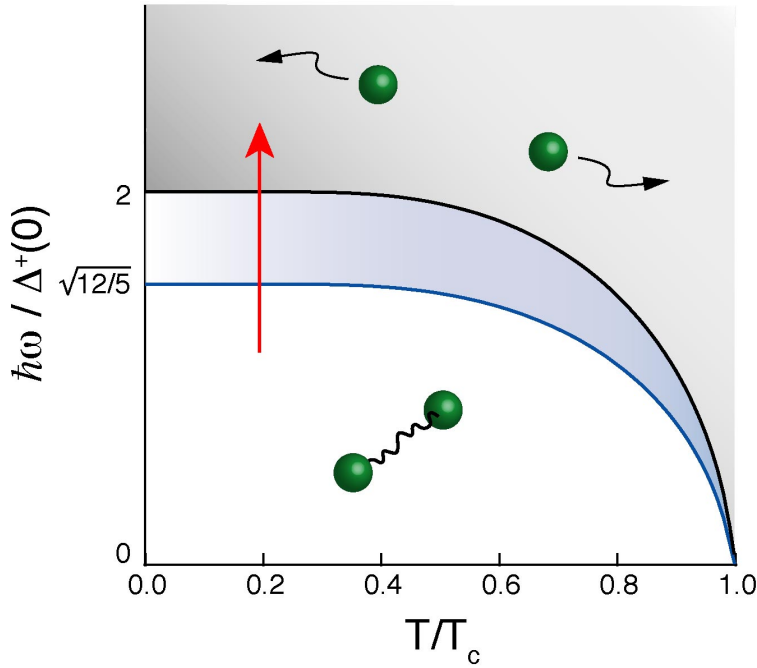


Fig. 1 (Color on-line). Schematic of the threshold energy for pair-breaking (black curve) and the ISQ-mode (blue curve) as a function of temperature normalized to the transition temperature. The shaded blue region is the only region in which transverse sound propagates. Decreasing the pressure at low temperature (pressure sweep technique) sweeps the acoustic wave energy relative to the gap energy, represented by the red arrow. The shaded black region is the particle-hole continuum identified schematically by independent quasiparticles. Below the black curve, they are shown as a bound Cooper pair.

Fig. 2. Hence, the acoustic response is sensitive to: the phase velocity, proportional to the period between the acoustic response oscillations; attenuation, increasing with decreasing amplitude of the acoustic response oscillations and proportional to b ; and the polarization of the transverse sound wave. We work from 76 to 170 MHz, the 13th to 29th harmonics of the transducer. The 17th harmonic of our *AC*-cut transducer, generates primarily longitudinal sound, likely from a slightly miscut transducer. This allows us to perform longitudinal sound measurements with the high resolution in frequency and the sensitivity of a shear transducer and directly compare longitudinal and transverse acoustic response traces. The acoustic response for longitudinal sound is similar to that of Eq. 1, but without the polarization ($\cos \theta$) factor and with c corresponding to the velocity of longitudinal sound.

We show in Fig. 2 representative energy (pressure) sweeps using both transverse and longitudinal acoustic response as a function of energy normalized to the weak-coupling-plus gap [3,20]. The green arrow indicates the energy of the 2Δ -mode, $\hbar\Omega_{2\Delta}$, in the transverse sound trace. The 2Δ -mode was identified by changes in the transverse phase velocity, attenuation and

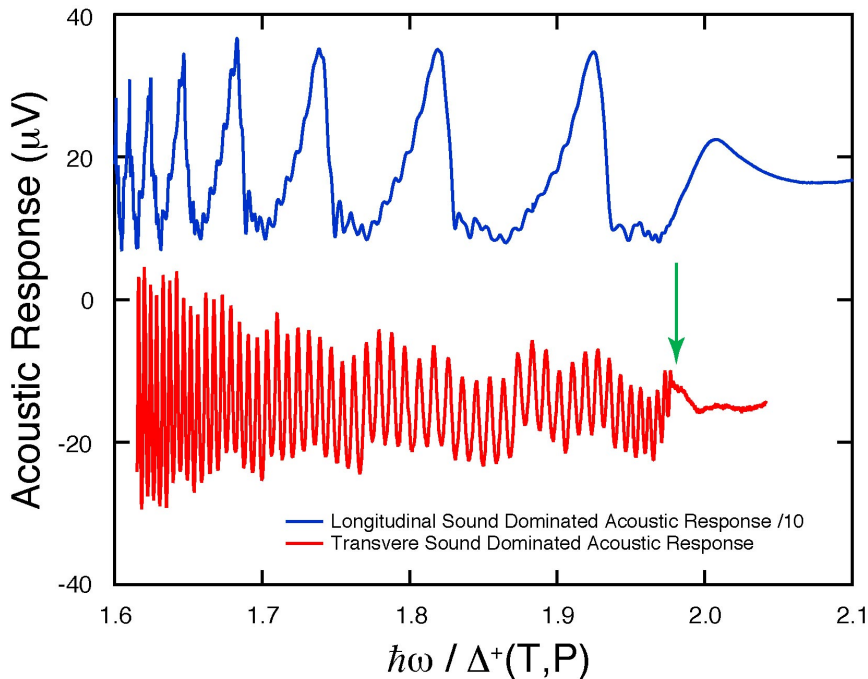


Fig. 2 (Color on-line). Transverse acoustic response oscillations (lower red trace) at $\approx 550 \mu\text{K}$ and longitudinal acoustic response oscillations (upper blue trace) at $\approx 600 \mu\text{K}$ as a function of energy normalized to the weak-coupling-plus gap. The background has been subtracted from the transverse trace to facilitate comparison. The frequency of transverse sound in the lower trace is 88 MHz and is 99.8 MHz for the longitudinal sound in the upper trace. The green arrow indicates the position of the 2Δ -mode, which is below $2\Delta^+(0)$ at the pressure corresponding to this trace. For the upper trace a modulation of approximately 10% corresponds to transverse sound. Conversely, longitudinal sound is weakly generated in the lower trace.

acoustic birefringence [8]. Further analysis of the attenuation of transverse sound is discussed elsewhere [23]. We do not see a dramatic change in the phase velocity of the longitudinal trace near pair-breaking in Fig. 2 that would indicate coupling to this, or any other, collective mode. The small oscillations in the longitudinal trace are from transverse acoustic response that is generated in addition to longitudinal sound.

For each full oscillation in the acoustic response, as in the lower trace in Fig. 2, one half wavelength of the transverse standing wave has entered or left the cavity as described by Eq. 1. Therefore the velocity difference between each maximum (minimum) corresponds to a half wavelength and we convert the period of the acoustic response oscillations into the change in the phase velocity as a function of pressure, Δc , where $(\Delta c/c)^{-1} = \frac{D\omega}{\pi c} - 1$. Absolute values for the transverse sound phase velocity, $c_t = c$, can then be obtained by fixing the velocity at one particular frequency, which we take to be the phase velocity approaching the ISQ-mode, through comparison with calculations based on the theoretical dispersion relation for transverse sound

[4]. This dispersion relation in the long wavelength limit and zero magnetic field [4, 24] is given by:

$$\frac{\omega^2}{q^2 v_F^2} = A_0 + A_{2-} \frac{\omega^2}{\omega^2 - \Omega_{2-}^2 - \frac{2}{5} q^2 v_F^2}, \quad (2)$$

where v_F is the Fermi velocity and q is the complex wavevector,

$$q = k + i\alpha, \quad (3)$$

k is the real wavevector, α is the attenuation, and the phase velocity is $c_t = \omega/k$. The ISQ-mode frequency closely follows the temperature and pressure dependence of the energy gap, $\Delta(T, P)$:

$$\Omega_{2-}(T, P) = a_{2-}(T, P)\Delta(T, P), \quad (4)$$

where $a_{2-} \approx \sqrt{12/5}$. For the precise values of a_{2-} we use those determined experimentally in Refs. [6, 7]. The first term on the right hand side of Eq. 2 is the quasiparticle background, the contribution to the dispersion in the absence of off-resonant coupling to the ISQ-mode,

$$A_0 = \frac{F_1^s}{15} (1 - \lambda) \left(1 + \frac{F_2^s}{5}\right) / \left(1 + \lambda \frac{F_2^s}{5}\right). \quad (5)$$

The second term on the right hand side of Eq. 2 gives the off-resonant coupling of transverse sound to the ISQ with strength:

$$A_{2-} = \frac{2F_1^s}{75} \lambda \left(1 + \frac{F_2^s}{5}\right)^2 / \left(1 + \lambda \frac{F_2^s}{5}\right). \quad (6)$$

Here we have included all Fermi liquid terms, F_l^s , for $l \leq 2$. The Tsuneto function, $\lambda(\omega, T)$, can be thought of as a frequency dependent superfluid stiffness [4] and is numerically calculated using the weak-coupling-plus gap [20], $\Delta^+(T, P)$, tabulated by Halperin and Varoquaux [3].

The agreement between the above theoretical dispersion relation and the data is excellent for energies below $\sim 1.8\Delta^+$. To fit the sound velocity above this energy we add a term to the dispersion, Eq. 2, which corresponds to coupling of the 2Δ -mode to transverse sound, with coupling strength, $A_{2\Delta}$:

$$\frac{\omega^2}{q^2 v_F^2} = A_0 + A_{2-} \frac{\omega^2}{\omega^2 - \Omega_{2-}^2 - \frac{2}{5} q^2 v_F^2} + A_{2\Delta} \frac{1}{\omega^2 - \Omega_{2\Delta}^2}. \quad (7)$$

This form neglects the width of the collective modes, as well as dispersion corrections to the 2Δ -mode energy, since it has not yet been calculated. The calculated velocity from this phenomenological dispersion relation fits the data precisely, shown in Fig. 3, with coupling strength, $A_{2\Delta} = 0.18$ for the 88 MHz data (red curve) and $A_{2\Delta} = 0.15$ for the 111.5 MHz data (green curve). At the higher frequency (which corresponds to higher pressures) the transverse sound velocity is slightly lower over most of the energy range. This is in contrast with the longitudinal sound velocity, c_l , which increases with increasing pressure [3]. Near pair-breaking $c_t = 66.1$ m/s at 2.4 bar and 88 MHz, and $c_t = 62$ m/s at 5.6 bar and 111.5 MHz. These values scale with

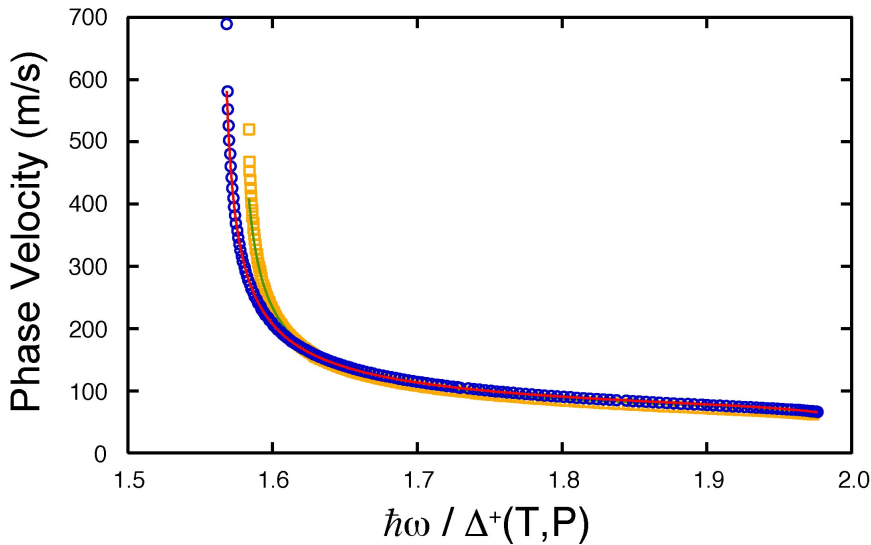


Fig. 3 (Color on-line). Phase velocity of transverse sound as a function of energy normalized to the weak-coupling-plus gap at low temperature ($\approx 550 \mu\text{K}$). The blue circles are at 88 MHz and the orange squares are at 111.5 MHz. The red curve is the theoretical phase velocity for 88 MHz with the new dispersion term and the green curve is for 111.5 MHz.

the Fermi velocities of 54.8 m/s and 50.3 m/s at 2.4 and 5.6 bar respectively, being $\approx 22\%$ larger than the Fermi velocity near the frequency $\omega \approx 2\Delta/\hbar$ in both cases.

In addition to coupling between transverse sound and the ISQ, there is also a coupling between longitudinal sound and the ISQ. Similar to the transverse case, this gives an increased longitudinal sound velocity and increased attenuation near the ISQ. The dispersion relation for longitudinal sound in superfluid ^3He is given by [4]

$$\frac{\omega^2}{q^2 c_1^2} = 1 + \frac{4}{15} \left(\frac{q v_F}{\omega} \right)^2 (1 - \lambda) + \frac{8}{75} \left(\frac{q v_F}{\omega} \right)^2 \lambda \left[\frac{\omega^2}{\omega^2 - \Omega_{2-}^2 - \frac{7}{15} q^2 v_F^2} \right], \quad (8)$$

where c_1 is the hydrodynamic sound velocity, $c_l = \omega/k$ is the phase velocity and $q = k + i\alpha$. Note that there are a few significant differences between Eq. 8 and Eq. 2. One very important difference is the first term on the right side of Eq. 8 that results in real valued solutions at frequencies below the ISQ where longitudinal sound is allowed to propagate. Additionally we find that there continues to be acoustic response oscillations in the longitudinal trace over all energies that we could measure even above pair-breaking, shown in Fig. 4.

The longitudinal acoustic response oscillations can be converted to velocity and attenuation as was done for transverse sound [8, 23]. This is shown in Fig. 5. The sound velocity, Fig. 5a, calculated from the theoretical dispersion relation, Eq. 8, is given by the blue curve. The data is then fixed to the

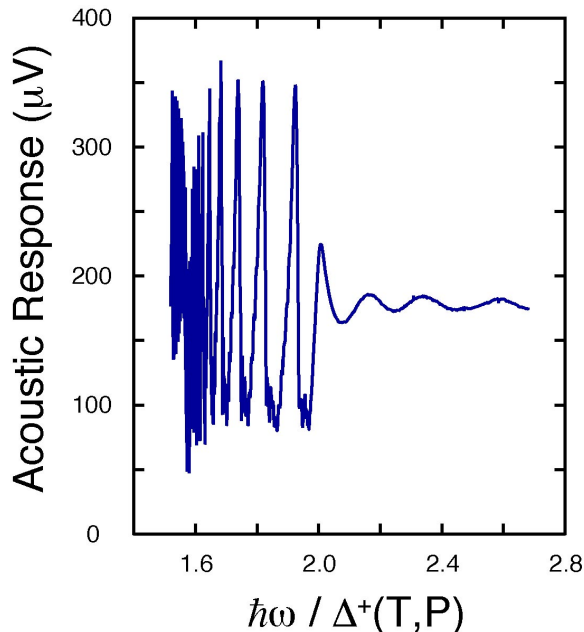


Fig. 4 (Color on-line). Longitudinal acoustic response oscillations as a function of energy normalized to the weak-coupling-plus gap at low temperature ($\approx 600 \mu\text{K}$) at 99.8 MHz. The amplitude of the oscillations decreases above $\approx 2\Delta^+$, but they continue to the highest energies, indicating that longitudinal sound propagates well into the particle-hole continuum.

theoretical velocity near the ISQ-mode, thus determining the longitudinal sound velocity at all other energies (gold circles). The theory and data are in good agreement over the entire energy range. The pressure dependence of the longitudinal sound velocity in the normal state, c_1 as tabulated in Ref. [3], is given as the dashed black curve in Fig. 5a. It is interesting to note that the dominant contribution to the energy dependence of the longitudinal sound velocity, at all energies other than near the ISQ-mode, comes from its dependence on pressure during the pressure sweep. Moreover, there seems to be no strong effect on the longitudinal sound velocity near the pair-breaking energy where we have evidence for a new mode from transverse sound, possibly because of the low resolution in energy in this measurement. This is the first measurement of the phase velocity of longitudinal sound for such high attenuation, which has been facilitated in our case by using a narrow cavity and acoustic interference techniques.

Furthermore, we can determine the relative attenuation of longitudinal sound from the amplitude of the acoustic response oscillations, shown in Fig. 5b. It is reasonable to expect that the attenuation of longitudinal sound is nearly zero away from the ISQ-mode and pair-breaking [25], which would mean that the relative attenuation in Fig. 5b is nearly the absolute attenuation. The energy resolution of this attenuation data is rather poor owing to the short acoustic path length, but extends to $\approx 10\times$ the attenuation

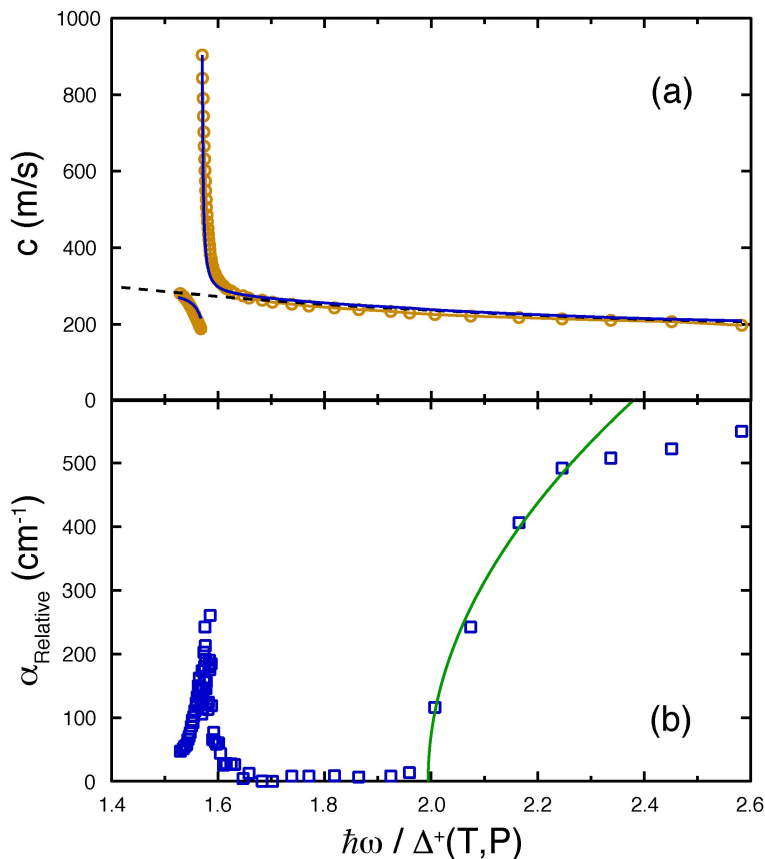


Fig. 5 (Color on-line). Longitudinal sound velocity (a) and attenuation (b) as a function of energy normalized to the weak-coupling-plus gap at low temperature ($\approx 600 \mu\text{K}$) at 99.8 MHz. In the upper panel the theoretical sound velocity is given by the blue curve and the data by the gold circles. The pressure dependence of the longitudinal sound velocity in the absence of coupling to the ISQ-mode is given by the dashed black curve. In the lower panel the relative attenuation of longitudinal sound is given as the blue squares. The green curve is a fit to Eq. 9, giving $2\Delta_{\text{pair-breaking}} = (1.994 \pm 0.006)\Delta^+$.

of previous measurements, which allows us to determine the attenuation at energies far above pair-breaking. Unlike the longitudinal sound velocity, the attenuation shows a dramatic effect near the threshold energy. It is expected [19] that the attenuation from pair breaking behaves as

$$\alpha \sim \sqrt{\hbar\omega - 2\Delta_{\text{pair-breaking}}}. \quad (9)$$

Fitting our data to this relation, the green curve in Fig. 5b, yields $2\Delta_{\text{pair-breaking}} = (1.994 \pm 0.006)\Delta^+$. At even higher energies, the attenuation deviates from this relation, which is not understood. The nature of sound propagation deep into the particle-hole continuum and at low temperatures is not well-established, perhaps in part since there have been no experimental

results until this work. In this spirit we note that the experimental conditions exceed the quantum limit described by Landau [1] in his discussion of zero sound propagation in the normal Fermi liquid. In our case we have $\hbar\omega/2\pi k_B T \sim 1.3$. It is in this low temperature limit, so far unexplored theoretically at high frequency in superfluid ^3He , that the quantum mechanical form of the quasiparticle distribution function should be used. In the normal Fermi liquid it results in sound attenuation, even at zero temperature.

3 Lower Limits on the Pair-Breaking Energy

The single most fundamental quantity in the thermodynamic description of both superconductors and superfluid ^3He is the gap energy, $\Delta(T)$. Understanding the gap energy of superfluid ^3He is vital for correct interpretation of collective mode frequencies, which scale with the gap, as well as virtually all static properties of the superfluid. The energy gap is the energy per quasiparticle required to dissociate a Cooper pair into its constituent quasiparticles. Anisotropy in the gap as well as strong coupling corrections to the free energy can in principle increase the gap energy above $\Delta(0) = 1.764k_B T_c$. Acoustic measurements of the energy gap are based on the principle that its signature is a sharp onset of attenuation associated with pair-breaking. Previous measurements of the pair breaking energies using longitudinal sound have indicated anomalously low values for the energy gap, below the $1.764k_B T_c$ of BCS theory [9,10]. In order to investigate this surprising result, we use the 2Δ -mode as a lower bound on the pair-breaking energy of superfluid ^3He . By doing this, we establish lower limits on the energy of the gap, which we find to be above the weak-coupling BCS theory at all pressures.

In this light, the results of Movshovich *et al.* [9] and Masuhara *et al.* [10] from longitudinal sound measurements, are particularly unsettling since both of these experiments yield gap energies below Δ_{BCS} , at low pressures. To date, these two experiments are the only ones to have measured the gap at low temperatures, below $T/T_c < 0.5$. Other experiments [25,26,27] measured the pair breaking edge using attenuation of longitudinal sound near T_c . Adenwalla *et al.* [28] used longitudinal acoustics to identify a feature with 2Δ down to $T/T_c \approx 0.6$. These experiments were consistent with the weak-coupling-plus model [20] when combined with the temperature scale of Greywall [21] but are not sensitive tests of the low temperature limit of the weak-coupling-plus theory [20].

Our measurement of $\hbar\Omega_{2\Delta}$, using transverse acoustic response is the first experiment using transverse sound to shed light on the gap. The off-resonant coupling of transverse sound to the ISQ-mode is extinguished above pair-breaking and transverse sound no longer propagates by this mechanism [4]. This is expected to behave like a step-function, sharply increasing the attenuation and making transverse sound well-suited for measuring pair-breaking. The only problem with this scenario is the appearance of the 2Δ -mode [8]. Nonetheless, using the 2Δ -mode as a *lower bound*, we can draw conclusions about the pair-breaking energy. Comparing the transverse and longitudinal traces, Fig. 2, it is clear that transverse sound does not propagate above pair-breaking in our acoustic cavity. It is widely believed that transverse sound

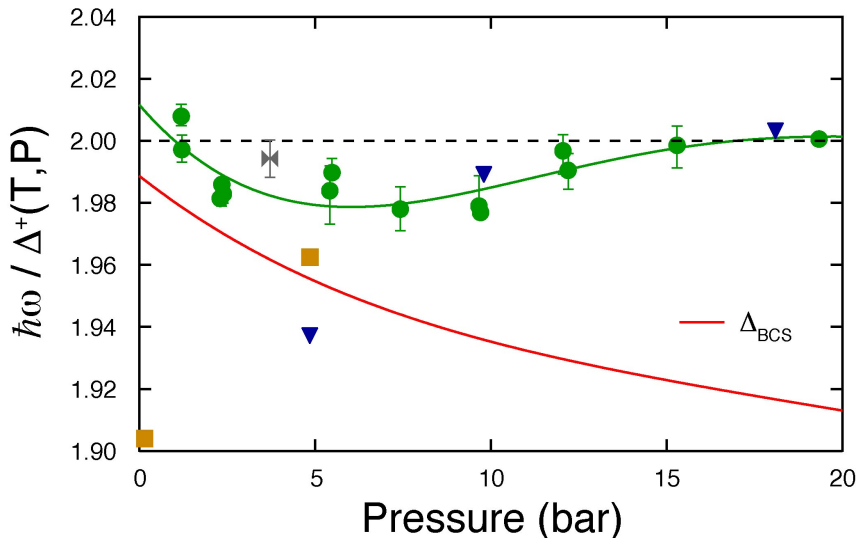


Fig. 6 (Color on-line). Measurements of $\hbar\Omega_{2\Delta}$, green circles, normalized to the gap at zero temperature in the weak-coupling-plus model as a function of pressure. The green line is a fit to the data, Eq. 13. The grey bow-tie is from the attenuation of longitudinal sound. The black dashed line is the weak-coupling-plus gap [20]. The red line is the BCS weak-coupling gap [3]. The blue downward triangles are the data of Movshovich *et al.* and the gold squares are the data of Masuhara *et al.* We find an upturn at low pressures for the minimum value for 2Δ , as opposed to the precipitous drop to lower values for the data of Movshovich *et al.* and Masuhara *et al.*

should propagate in the normal state [1], but we have found that the attenuation is too high for us to observe standing waves with the acoustic path length used here, $2D = 63.1 \mu\text{m}$.

Fig. 6 shows the results of our $\hbar\Omega_{2\Delta}$ measurements, normalized to the weak-coupling-plus gap, as a function of pressure. We find $\hbar\Omega_{2\Delta}$ is within $\approx 1\%$ of the expected value of the weak-coupling-plus gap for $\lesssim 20$ bar and our interpretation is that the gap energy *never* falls below Δ_{BCS} . Our measurement of the pair-breaking threshold energy extracted from longitudinal sound attenuation is shown as the grey bow-tie in Fig. 6 and is consistent, in that it lies at an energy above the measurements of $\hbar\Omega_{2\Delta}$. There is good agreement at pressures ≥ 10 bar between our measurements and those of Movshovich *et al.* [9], but in our results there is a clear upturn at the lowest pressures in stark contrast to the experiments of both Movshovich *et al.* [9] and Masuhara *et al.* [10]. It is possible that Movshovich *et al.* are detecting an increased attenuation coming from the feature observed by Ling *et al.* [25] that couples to longitudinal sound and resides near 2Δ in a magnetic field, although its exact origin is unknown [29,30], since their experiment involved sweeping the magnetic field to move the gap energy through their acoustic spectrum. The results of Masuhara *et al.* are not subject to this source of ambiguity and it is difficult for us to reconcile their experiment with ours.

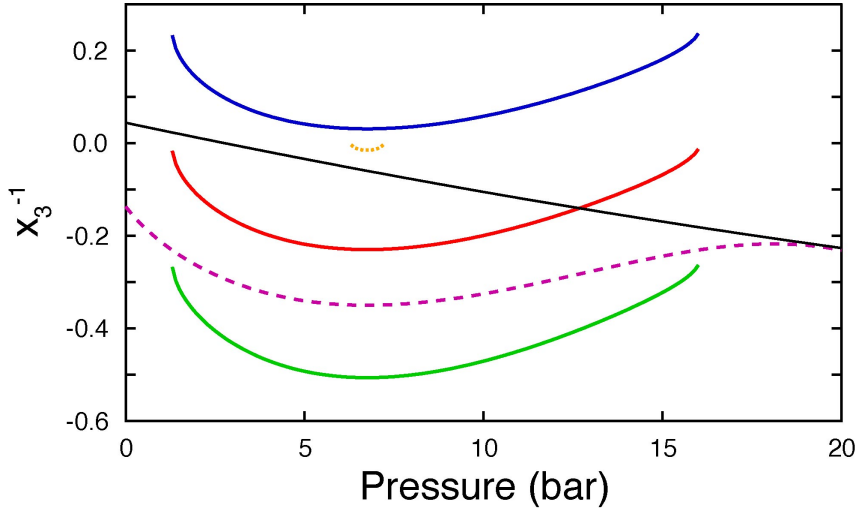


Fig. 7 (Color on-line). f -wave pairing interaction strength from 2Δ -mode energies using Eq. 11. The red curve uses $F_4^s = 0$, the blue curve $F_4^s = -1$ and the green curve $F_4^s = +1$. The purple dashed curve results from $F_4^s = 0$ and increasing T_c (and therefore Δ^+) by 1%, and the orange dotted curve results from $F_4^s = 0$ and decreasing T_c by 1%. Whenever $\Omega_{4^-} \geq 2\Delta^+$ the Tsuneto function is imaginary and there are no solutions to Eq. 11. The black line represents the the values of x_3^{-1} from Fraenkel *et al.* [17].

4 Extraction of f -Wave Pairing and Fermi Liquid Interactions

Predictions for the $J = 4^-$ mode frequency, Ω_{4^-} , depend on the existence of an attractive f -wave pairing interaction [11], as well as the unknown Fermi liquid parameter, F_4^s . Parameterization of the f -wave pairing strength is given by

$$x_3^{-1} = \frac{1}{v_1^{-1} - v_3^{-1}}, \quad (10)$$

where v_1 and v_3 are the pairing potentials due to p -wave and f -wave interactions respectively. Attractive f -wave pairing interactions correspond to negative values for x_3^{-1} , and x_3^{-1} is zero if the f -wave pairing interaction is zero. Repulsive interactions give a positive x_3^{-1} . The predicted $J = 4^-$ mode frequency in terms of x_3^{-1} and F_4^s is given by [13]:

$$\left(1 + \frac{1}{9}F_4^s\lambda\right) + x_3^{-1}\lambda\left[\frac{\Omega_{4^-}^2}{4\Delta^2} - \frac{5}{9} + \frac{5}{81}F_4^s\left(\frac{\Omega_{4^-}^2}{4\Delta^2} - 1\right)\lambda\right] = 0, \quad (11)$$

for the case when $x_5^{-1} = 0$ (zero h -wave pairing interactions).

Evaluation of the strength of f -wave pairing interactions from the measured values for the energy of the 2Δ -mode is complicated by the fact that there is no experimental information on F_4^s . Nonetheless, we can evaluate Eq. 11, for various constant values of F_4^s . Specifically in the case where $F_4^s = 0$

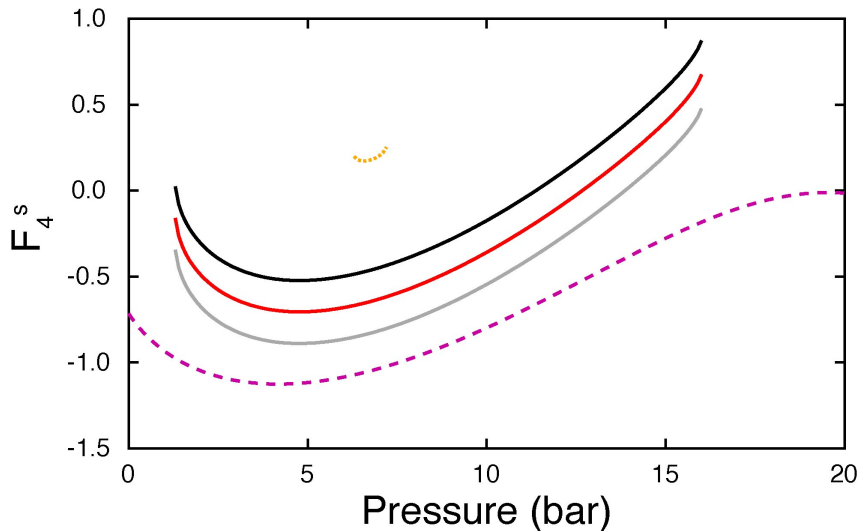


Fig. 8 (Color on-line). F_4^s calculated from Eq. 11 using $\Omega_{2\Delta}$ -mode energies and x_3^{-1} from RSQ-mode energies [17,18] (red curve). F_2^a is not particularly well known [3] and alteration of F_2^a by ± 0.2 yields x_3^{-1} , which give the black and grey curves, respectively. The purple dashed curve results from increasing T_c by 1%, and the orange dotted curve results from decreasing T_c by 1%.

we can rewrite Eq. 11 as

$$x_3^{-1} = \left[\lambda \left(\frac{\Omega_{4-}^2}{4\Delta^2} - \frac{5}{9} \right) \right]^{-1}. \quad (12)$$

For Ω_{4-} in Eq. 12, we use our values from the 2Δ -mode [8] given up to 20 bar by:

$$\hbar\Omega_{2\Delta}(T, P) = 2\Delta^+(T, P)(1.006 - 6.7 \times 10^{-3}P + 8.7 \times 10^{-4}P^2 - 3.94 \times 10^{-5}P^3 + 6 \times 10^{-7}P^4). \quad (13)$$

The values of x_3^{-1} extracted from this analysis are presented in Fig. 7. When $\Omega_{4-} \geq 2\Delta^+$ the Tsuneto function is imaginary and there are no solutions to Eq. 11. The values of x_3^{-1} are sensitive to the energy of the collective mode normalized to the pair-breaking energy, $\Omega_{4-}/2\Delta^+$. Since the energy gap is proportional to T_c , uncertainty in the absolute temperature will affect these values. The uncertainty in T_c was estimated by Greywall to be $\pm 1\%$ [21] and we show the result of adjusting T_c by $\pm 1\%$ as the purple dashed and orange dotted curves respectively. The effect of T_c on λ was taken into account.

These values for x_3^{-1} in Fig. 7 are inconsistent with the values we extracted from measurements of the frequency and Zeeman splitting of the ISQ-mode [6,7]. However, as was noted previously, the effect of interactions on the ISQ mode frequency, and possibly the Zeeman splitting of this mode, are likely affected by strong coupling corrections which are of comparable magnitude

[6,7]. On the other hand, the effect of x_3^{-1} on the RSQ-mode energies as reported by Fraenkel *et al.* [17,18] is an order of magnitude larger than for the ISQ-mode energies and as a consequence, they are possibly less affected by strong-coupling corrections. Therefore, using the RSQ-mode values of x_3^{-1} and using the $\Omega_{2\Delta}$ -mode energies, it is possible to give possible values for F_4^s from Eq. 11. These values are given as the red curve in Fig. 8. Unfortunately, the relevant Fermi liquid parameter, F_2^a , for calculation of x_3^{-1} from the RSQ-mode energies is not well known [3]. Increasing and decreasing F_2^a by 0.2 yields x_3^{-1} given by the black and grey curves respectively in Fig. 8. The purple dashed curve results from increasing T_c by 1%, and the orange dotted curve results from decreasing T_c by 1%. Landau's formulation of interactions in ^3He in terms of a strongly converging expansion in Legendre polynomials with coefficients, F_l , would lead us to expect that the Fermi liquid parameters, F_l , should decrease rapidly as l increases. According to the analysis above the absolute values of F_4^s might be comparable to, or larger than, those of F_2^s [3].

5 Conclusions

We have shown that low temperature pressure sweeps are a high resolution technique to study the energy dependence of longitudinal and transverse sound in superfluid $^3\text{He-B}$, without the complicating effects of thermal damping that occur in temperature sweeps. This allows measurement of the absolute values for the phase velocity of both longitudinal and transverse sound as a function of energy. These measurements reveal the coupling of transverse sound to a collective mode near the pair-breaking edge, the 2Δ -mode, which is likely the $J = 4^-$ mode. We use the 2Δ -mode energies, in combination with the attenuation of longitudinal sound, to set lower limits on the energy of pair-breaking. We conclude that pair-breaking never falls below the value given by weak-coupling BCS theory. Additionally, we use the energies of this mode to estimate the strength of sub-dominant f -wave pairing interactions.

Future experiments with magnetic fields should bring the energy of pair-breaking below that of the 2Δ -mode, because of the large difference in their Zeeman splittings [8,31]. This would allow direct measurement of the pair-breaking energy using transverse sound, which could then be extrapolated to zero magnetic field. Direct measurement of the energy of pair-breaking, with the precision of high frequency transverse acoustics, can provide narrow constraints on the *absolute* temperature scale.

Acknowledgments

We acknowledge support from the National Science Foundation, DMR-0703656 and thank J.A. Sauls, C.A. Collett, W.J. Gannon and S. Sasaki for useful discussions.

References

1. L.D. Landau, Sov. Phys. JETP **32**, 59 (1957).
2. W.R. Abel, A.C. Anderson and J.C. Wheatley, Phys. Rev. Lett. **17**, 74 (1966).
3. W.P. Halperin, E. Varoquaux, in *Helium Three*, ed. by W.P. Halperin and L.P. Pitaevskii (Elsevier, Amsterdam 1990).
4. G.F. Moores, J.A. Sauls, J. Low Temp. Phys. **91**, 13 (1993).
5. Y. Lee, T.M. Haard, W.P. Halperin and J.A. Sauls, Nature **400**, 431 (1999).
6. J.P. Davis, H. Choi, J. Pollanen and W.P. Halperin, Phys. Rev. Lett. **97**, 115301 (2006).
7. J.P. Davis, H. Choi, J. Pollanen and W.P. Halperin, Phys. Rev. Lett. **100**, 015301 (2008).
8. J.P. Davis, J. Pollanen, H. Choi, J.A. Sauls, W.P. Halperin, Nature Physics **4**, 571-575 (2008).
9. R. Movshovich, N. Kim, D.M. Lee, Phys. Rev. Lett. **64**, 431 (1990).
10. N. Masuhara, B.C. Watson, M.W. Meisel, Phys. Rev. Lett. **85**, 2537 (2000).
11. J.A. Sauls, Phys. Rev. B **34**, 4861 (1986).
12. M. Fogelström, D. Rainer, J.A. Sauls, Phys. Rev. Lett. **79**, 281-284 (1997).
13. J.A. Sauls, J.W. Serene, Phys. Rev. B **23**, 4798 (1981).
14. R.S. Fishman, Phys. Rev. B **36**, 79 (1987).
15. R.S. Fishman, J.A. Sauls, Phys. Rev. B **38**, 2526 (1988).
16. J.A. Sauls, J.W. Serene, Phys. Rev. Lett. **49**, 1183 (1982).
17. P.N. Fraenkel, R. Keolian, J.D. Reppy, Phys. Rev. Lett. **62**, 1126 (1989).
18. P.N. Fraenkel, Thesis (Cornell University) unpublished (1990).
19. R.H. McKenzie, J.A. Sauls, in *Helium Three*, ed. by W.P. Halperin and L.P. Pitaevskii (Elsevier, Amsterdam 1990).
20. D. Rainer, J.W. Serene, Phys. Rev. B **13**, 4745 (1976).
21. D.S. Greywall, Phys. Rev. B **33**, 7520 (1986).
22. P.J. Hamot, Thesis (Northwestern University) unpublished (1994).
23. J.P. Davis, H. Choi, J. Pollanen, W.P. Halperin, submitted to Phys. Rev. Lett. (2008). [arXiv: 0807.2221]
24. J.A. Sauls, in *Topological Defects and the Non-Equilibrium Dynamics of Symmetry Breaking Phase Transitions*, ed. by Y.M. Bunkov and H. Godfrin (Kluwer Academic, Dordrecht 2000). (cond-mat/9910260)
25. R. Ling, J. Saunders, E.R. Dobbs, Phys. Rev. Lett. **59**, 461 (1987).
26. R.W. Gianetta, A. Ahonen, E. Polturak, J. Saunders, E.K. Zeise, R.C. Richardson, D.M. Lee, Phys. Rev. Lett. **45**, 262 (1980).
27. M.W. Meisel, B.S. Shivaram, B.K. Sarma, J.B. Ketterson, W.P. Halperin, Phys. Lett. A **98**, 437 (1983).
28. S. Adenwalla, Z. Zhao, J.B. Ketterson, B.K. Sarma, Phys. Rev. Lett. **63**, 1811 (1989).
29. R.H. McKenzie, J.A. Sauls, J. Low Temp. Phys. **90**, 337 (1993).
30. M. Ashida, J. Hara, K. Nagai, J. Low Temp. Phys. **105**, 221 (1996).
31. N. Schopohl, L. Tewordt. *J. Low Temp. Phys.* **45**, 67 (1981).